

Experimental investigation of mixing in a novel continuous chaotic mixer

Seyyed Mostafa Hosseinalipour^{*,†}, Amir Tohidi^{*}, Payam Rahim Mashaei^{*}, and Arun Sadashiv Mujumdar^{*****}

^{*}CFD and CAE Laboratory, Department of Mechanical Engineering, Iran University of Science and Technology, Narmak, Tehran, Iran

^{**}Institute of Chemical Technology, Mumbai, India

^{***}Chemical & Biomolecular Engineering Department, Hong Kong University of Science & Technology, Hong Kong
(Received 21 April 2013 • accepted 27 February 2014)

Abstract—This paper presents and discusses results of an experimental study of laminar mixing of a highly viscous fluid (dough) in a continuous chaotic mixer. The mixer consists of an eccentric rotor that rotates co-axially within a stator, which results in chaotic advection. A dye injection technique was used to measure the mixing performance of the mixer. A mixing index was defined and computed by image processing of photographs of the exiting fluid from the mixer. Mixing characteristics were determined for constant as well as stepwise rotation of the rotor. Results revealed that mixing performance improves with increase in the rotational speed for constant rotational speed. The stepwise rotation case displayed better mixing performance than the constant speed case for stepwise changes of the amplitude as well as frequency of rotation.

Keywords: Dough Mixer, Highly Viscous Fluids, Chaotic Advection, Mixing, Laminar

INTRODUCTION

Mixing is usually an important part of many industrial processes, such as blending of ingredients, reactants in chemical reactors, addition of energy to create or break molecular bonds. Mixing of highly viscous materials is of particular interest in food processing [1].

Although mixing is widely used, a fundamental understanding is still somewhat limited. It is the oldest unit operation, improved in incremental stages by empiricism. However, increasing demands on close control of product quality and the trend towards intensive automation of the mixing process, have emphasized the need for obtaining quantitative and predictive design capabilities to optimize the design and performance of mixers. Food materials are rheologically complex and are typically difficult to mix uniformly [2]. Wheat flour dough is an excellent example of a highly viscous food material that requires optimal mixing in bread manufacturing all over the globe [1].

Understanding and manipulating mixing processes requires knowledge of the physical mechanisms involved in fluid mixing. Chaotic advection is one of the most interesting mechanisms which has been examined in recent years to improve fluid mixing performance [3]. The theory related to creating chaotic advection in a flow domain by simple geometrical perturbations has recently attracted much attention. In chaotic flows, the very small distance between adjacent particles grows exponentially and this is the reason behind the application of these flows in the mixers. It also leads to elongation and exponential increase in the contact area of the fluid elements causing better mixing performance. This fact has motivated many recent studies [4].

The literature [6–20] contains a number of devices designed to enhance mixing. These fall into one of two categories: active mixers that exert some form of active control over the flow field using moving parts or varying pressure gradients, and passive mixers that utilize no energy input except for the inherent hydrodynamic mechanisms (pressure head or pump) used to drive the fluid flow at a constant rate [5].

Table 1 presents a brief history of selected relevant experimental works accomplished on chaotic mixers.

One of the active techniques by which chaotic advection is produced is by irregularity in the flow pattern of the stirrer or the moving part of the mixer created by periodic rotation of eccentric cylinders [21,22]. Ottino et al. [9] developed techniques to predict the chaotic dispersion of passive tracers in two-dimensional low Reynolds number flows. They presented the design of a flow apparatus which allowed for an unobstructed observation of the entire flow region.

Aref et al. [23] studied chaotic advection in the creeping flow regime in the annular region between two eccentric cylinders. They showed that chaotic advection can be produced whenever the kinematic equations of motion for passively advected particles give rise to a non-integrable dynamical system.

Ottino et al. [10] investigated the effect of shear-thinning viscosity on chaotic mixing when the kinematics first begins to deviate from Newtonian flow. Their computations were for a periodic flow between eccentric cylinders. They showed that small variations in the velocity field associated with non-Newtonian kinematics produce large effects in the chaotic advection of a passive tracer.

Ottino et al. [24] presented an experimental and computational investigation of mixing of a viscoelastic fluid in two-dimensional time-periodic flows generated in an eccentric cylindrical geometry. The objective was to investigate the impact of fluid elasticity on the morphological structures produced by the advection of passive tracers in chaotic flows. Their results indicate that elasticity can in-

[†]To whom correspondence should be addressed.

E-mail: Alipour@iust.ac.ir

Copyright by The Korean Institute of Chemical Engineers.

Table 1. Experimental works accomplished on chaotic mixers

| Author | Type of perturbation applied | Geometry |
|----------------------|---|---------------------|
| Ottino [6] | Temporally periodic perturbation of wall velocity | Cavity |
| Zumbrun [7] | Temporally periodic perturbation of wall velocity | Cavity |
| Ottino [8] | Moving wall | Baffled cavity flow |
| Ottino [9,10] | Temporally periodic perturbation of velocity in eccentric cylinders | Eccentric cylinders |
| Funakoshi [11] | Temporally periodic perturbation of velocity in eccentric cylinders | Eccentric cylinders |
| Acharya [12] | Spatially periodic perturbation | Coil |
| Peerhossaini [13,14] | Spatially periodic perturbation | Coil |
| Cox [15] | Rotating inner cylinder | Eccentric cylinders |
| Peerhossaini [16,17] | Spatially periodic perturbation | Twisted channel |
| Ottino [18] | spatial perturbation of blade angle | Single blade mixer |
| Muzzio [19] | Temporally periodic perturbation of blades velocity | Six blades mixer |
| Metcalfe [20] | Spatially periodic perturbation | Arc mixer |

crease or decrease the degree of regularity.

Rodrigo et al. [4] considered the flow inside an eccentric two-cylinder mixer. The geometry was composed of two rotating cylinders. The outer cylinder rotated at a constant speed, while the inner cylinder had a time variable sinusoidal speed. Their study confirmed enhancement of heat transfer by chaotic advection in this geometry.

Metcalfe and Lester [20] conducted research on mixing and heat transfer of highly viscous food products by continuous chaotic advection inside a duct and evaluated the performance of a rotated arc mixer for continuous mixing and heat transfer in highly viscous food products. Their results indicated that the rotated arc mixer benefited from chaotic advection for mixing and heat transfer of fluids under high viscosity (low Reynolds) conditions.

According to the literature, almost all of the previous investigations were focused on dough mixers and their efficiency. Only a few studies [25] investigated the dough mixer performance by evaluating the chaotic flow.

Couch et al. [26] conducted a modeling and experimental study on rotating flows of dough kneading in two different rotating cylindrical containers: one with one stirrer and the other with two stirrers. Using laser doppler anemometry to obtain the velocity vectors, they demonstrated good agreement between numerical and experimental flow fields. This can be an important parameter for the design process.

Couch et al. [27] also studied free surface flows of dough in a rotating cylindrical container both numerically and experimentally. They examined the horizontal and vertical configurations of the container at different angular velocities. Laser scatter technology and video capture technique were employed to simulate free surface conditions and to obtain the experimental stresses, respectively. Very good agreement was reported between the shape of free surfaces of dough experimental flow and numerical simulations.

Kokini et al. [1] examined the mixing ability of single screw and twin screw dough mixers using finite element simulation. They calculated the mixing performance of two-dimensional dough mixers, either single screw or twin screw, using PolyFlow software. The 2D twin screw dough mixer was reported to be the more efficient mixer.

Kokini et al. [28] proposed a computational method to obtain

simultaneous scale-up of mixing and heat transfer in single screw extruders by several parametric 3D non-isothermal numerical simulations. They conducted parametric numerical simulations by varying the screw geometric variables.

It is obvious that most efforts have been put in the flour dough mixing enhancement area, but fewer efforts have been put into study of chaotic mixers for this purpose. Hosseinalipour et al. [25] introduced a mixer that consists of an eccentric rotor that rotates co-axially within a stator, which results in chaotic advection. They developed a mathematical model to overcome the difficulties encountered in dynamic meshing and to find the required fluid particle trajectories for assessing the presence of chaotic advection in the proposed mixer. Lyapunov exponents were calculated to quantify the exponential divergence of the initially close state-space trajectories and identify the chaotic behavior of the system as well. The reported flow field was a combination of both chaotic and non-chaotic zones.

This study aims to investigate experimentally laminar mixing of highly viscous fluids in a continuous chaotic mixer, based on the idea first proposed by Hosseinalipour et al. [25]. To investigate the mixing behavior, the effects of the constant and stepwise angular velocity of the rotor on mixing efficiency were studied.

EXPERIMENTAL SET-UP

The chaotic mixer includes an eccentric helical rotor that rotates around the stator. This is in contrast with other eccentric cylinder studies in which the chaotic trajectories can be produced. The rotor is helical with 25 mm radius and 120 mm pitch. This rotor has eccentricity of 10 mm towards the axis of stator, which enables creation of chaotic advection. A cylinder with diameter of 80 mm has been used as stator. Therefore, the gap between rotor and stator will be variable in the range of 5-15 mm. Two bearings fix the rotor to the frame of the apparatus and a motor is used to rotate it.

The dough mixer configuration and cross section of the mixer are schematically illustrated in Figs. 1 and 2 where r_r , r_s and e are the radius of rotor's cross section area, the radius of stator and the eccentricity between rotor's axis and stator's axis, respectively.

The rotation speed range of the rotor in this mixer was 5-35 rpm with a 1.5 kW motor. A schematic diagram and a photograph of the experimental apparatus and setup are shown in Figs. 3 and 4,

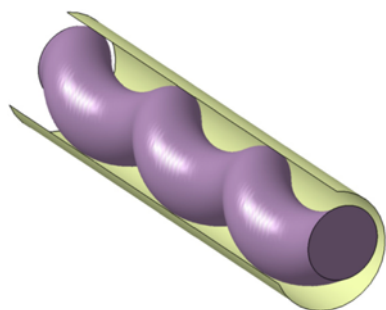


Fig. 1. Dough mixer configuration.

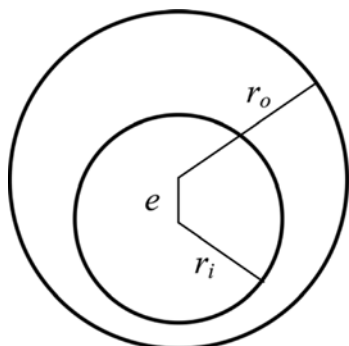


Fig. 2. Cross section of the mixer.

respectively.

To investigate the mixing performance of the dough mixer, 2 mL of dye was injected into the center of the mixer using an automatic injection system. A test tube with a length of 30 cm was attached to the mixer outlet. After removal of the test tube, fluid sampling was carried out. The colored fluid in the test tube was cut into 2 cm portions and their surfaces were photographed. Then mixing was quantitatively determined using image processing. The fluid patterns were recorded using a Panasonic Lumix DMC-FZ50 camera with 10.1-megapixel resolution.

1. Control of Rotor Rotational Speed

To control the rotor's rotational speed, a code was written which transmitted digital signals to a digital-to-analogue transformer card. Output analogue signals from this card with voltages in the range 0-10 V were sent to an inverter. The inverter transmitted an equivalent

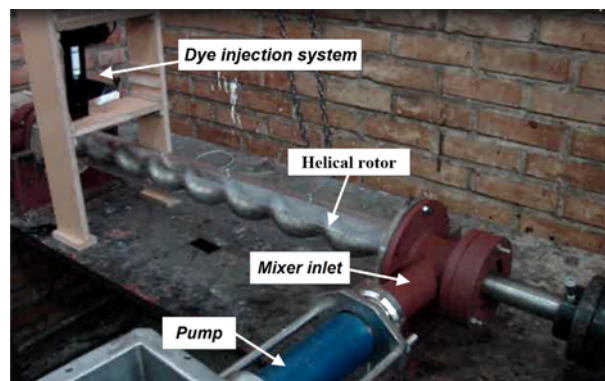


Fig. 4. Installation of parts of the dough mixer apparatus.

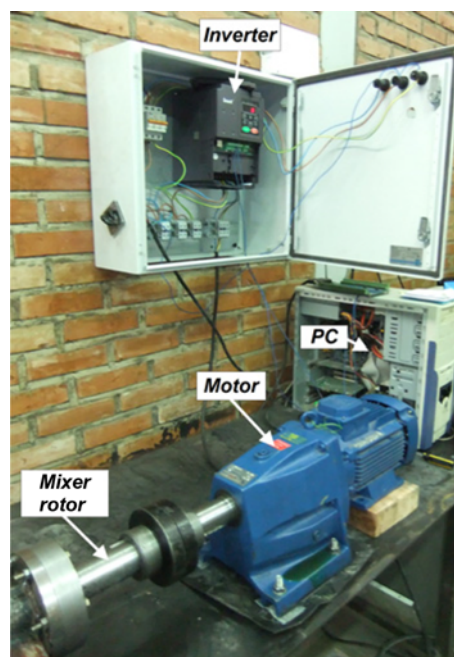


Fig. 5. Rotor rotational speed control system.

frequency analogous to the received voltage to the motor. This program has the capability to send protocols of constant and step-wise speed to the motor. Fig. 5 shows control system of rotor's rotational speed.

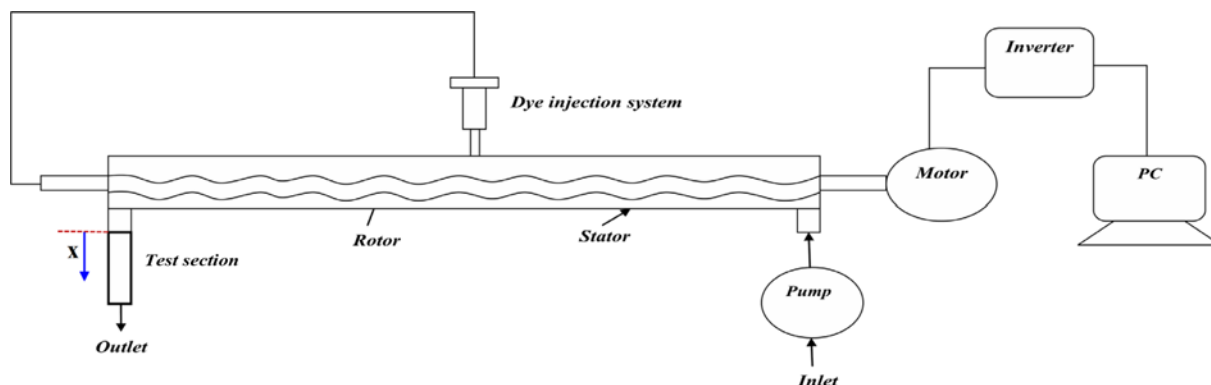


Fig. 3. Schematic view of installation of all parts of the dough mixer apparatus.

2. Injection System

To maintain identical injection conditions, a dye injection control system was used that transmitted commands through an infrared sensor to the microcontroller, while the injection was implemented by an inline engine. The dye injection control system included an infrared sensor, an Atmega16 micro-controller, an inline engine, and an injection syringe. This system enabled execution of the injection operation after data were acquired from the infrared sensor, including the number of shaft rotations inside the continuous mixer reaching the desired index. 2 mL of dye was injected into the mixer by adjusting the index properly.

3. Working Fluid

The first phase of the experimental work involved rheological characterization of dough in terms of the shear and dynamic properties. However, a viable model fluid was also required to be translucent to facilitate flow visualization and for this reason dilute polymer solutions were employed. Once suitable model fluids were developed, the subsequent phase of the experimental work was conducted for flow visualization in the model geometries [26]. The dilute polymer selected was carboxymethyl cellulose (CMC) solution in water with density of 1,000 kg/m³.

RESULTS AND DISCUSSION

Factors identified as being effective in mixing are rotor step, distance between rotor and stator, rotor motion protocols, and rotor rotation speed. We focused on the effects of mass flow rate and rotor motion protocols.

1. Rheological Properties of Working Fluid

The rheological properties of the fluids were characterized with a rheometer (Physica MCR 300). Parallel-plate geometry was used to determine the dynamic modulus. Fig. 6 depicts the shear viscosity obtained for dough and dilute CMC solutions from the same range of shear stress in which the dough mixer operated. The percentages represent the wheat flour content relative to the dough at 100%, i.e., “Dough 60%” represents 60% wheat flour and 40% water. Also, “CMC 1%” represent solution consists of 1% CMC and 99% water.

The CMC solutions showed similar shear thinning properties within

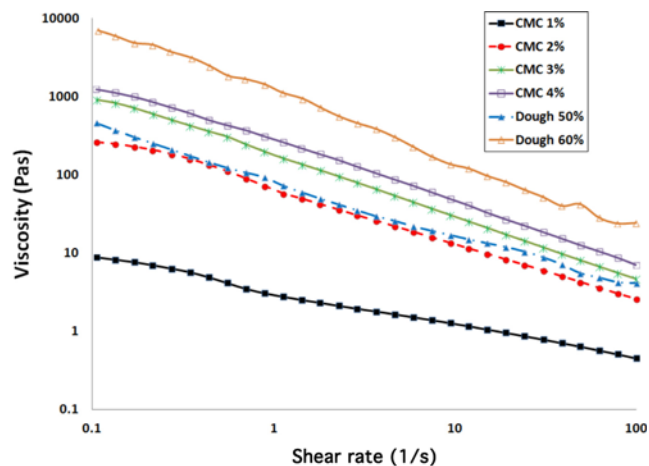


Fig. 6. Shear viscosity versus shear rate data for dough and diluted CMC solutions.

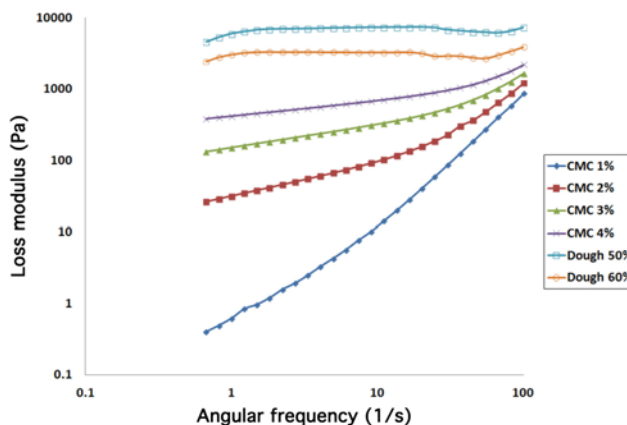


Fig. 7. Loss modulus data versus frequency for dough and CMC solutions.

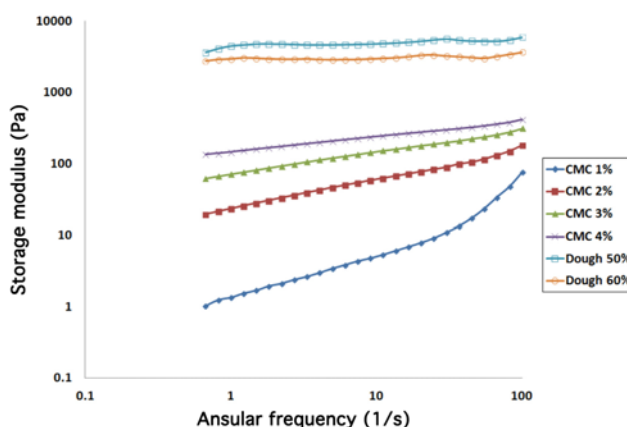


Fig. 8. Storage modulus data versus frequency for doughs and CMC solutions.

the measured range of shear rate and also proved a viscosity profile similar to that of dough.

Fig. 7 and Fig. 8 show corresponding dynamic data, storage modulus (G') and loss modulus (G''), for these materials.

The CMC solution exhibits similar trends to the dough, though the magnitudes of their dynamic moduli are considerably lower. It

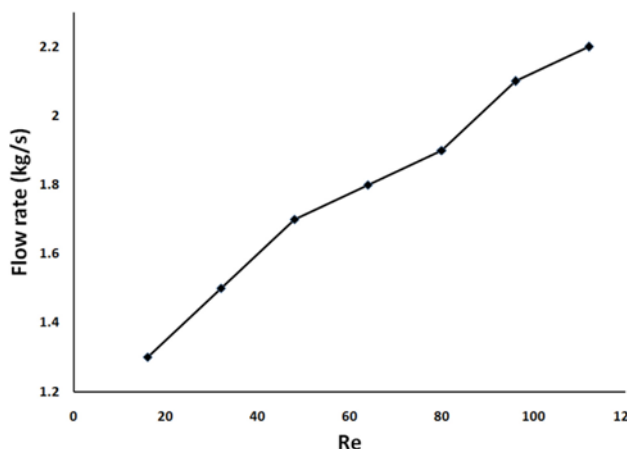


Fig. 9. Effect of rotor rotation speed on mixer's flow rate.

can be inferred from the graph that the dough itself is more elastic than viscose ($G' > G''$), while for the most dilute CMC solution the converse is true [26]. The 2% CMC solution was found to be the most suitable for flow visualization, while its shear thinning properties matches with dough 50% and also suitable candidate for the inelastic case.

Re numbers for flow in this geometry is defined as:

$$Re = \rho VL / \eta \tag{3}$$

where ρ , L , V and η are the density, mixer length, linear velocity of rotor and viscosity, respectively. For the model fluids under consideration, drive speeds of 5, 15, 25 and 35 rpm are applied, which correspond to Reynolds numbers of 16, 48, 78 and 110, respectively.

2. Mass Flow Rate

To study the effect of rotor speed on the mixer's output flow rate, mass flow rates were measured at various rotor rotation speeds. Fig. 9 shows that increase of the rotor rotation speed increases the dough mixer's rate of flow because of the higher propulsion force. Increasing the rotor rotation speed increases the rate of strain and dilutes the fluid as well, resulting in a decrease in pressure drop against the movement of the fluid.

3. Dough Tests

The experimental setup was used to investigate the water dough (50%) mixing. A series of tests were conducted using the injection of 2 mL red color dye as a passive tracer. Samples were provided using a very thin cutter to cut the exit dough at different elapsed times. Fig. 10 shows dough samples via time.

Photographs of each sample were analyzed to quantify the mixing of the red color in the dough. For each sampling it was necessary to switch off the mixer. The two main sources of error in the tests conducted were this enforced discontinuity in the sampling procedure and sample deformation.

To overcome the second problem, each sample was refrigerated immediately after sampling. Photographs were taken from samples after 8 hours when the final and fixed shape of sample was developed completely. The tracer diffusion in the sample during part of the freezing time resulted in an extra source of error in our measurements. As a conclusion, the conducted experiments for the water dough were not exact enough due to the difficulties reported above.

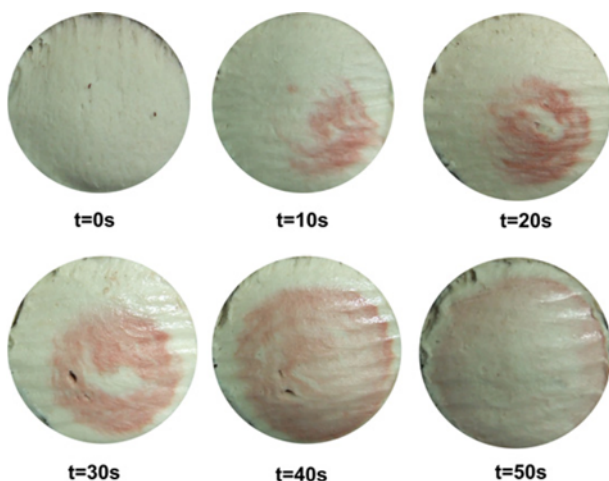


Fig. 10. Images for dough samples at Re=78.

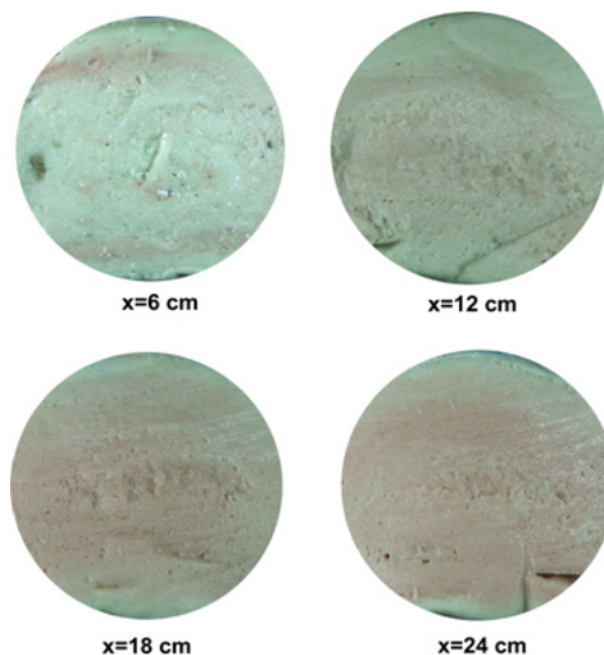


Fig. 11. Dough samples freezing.

Fig. 11 presents the output results for one of these tests.

4. CMC Tests

4-1. Effect of Rotor Rotational Speed

The effect of rotor rotational speed on the mixing characteristic of the mixer was investigated because this speed controls the mass flow rate of the fluid. To assimilate time quantity related to sampling implemented in the experiments, dimensionless time was used, calculated by:

$$t^* = \frac{m\Delta t}{t_0}$$

where t^* is dimensionless time for samplings done, m is number of the sample ($m=1, 2, \dots, 15$), Δt is time needed for 2 cm proceeding of flow through the test tube at desired rate of flow, and t_0 is time needed for 30 cm of flow to proceed through the tube at the desired rate of flow. Parameters of Δt and t_0 for each rate of flow were calculated and have been summarized in Table 2.

Fig. 12 shows images of the samples at Re=16. Clearly, poor mixing actually occurs at R=16; the dye is not able to reach center of flow after creating a pale loop. The dye has black color, which its distribution illustrates mixing performance. As seen in Fig. 12, black color has poor distribution versus dimensionless time. Although black color can be seen at center, it is distributed mostly around the test section.

The injected dye tended to maintain its direct path and not to rotate

Table 2. Parameters for calculating the dimensionless time

| t_0 (s) | Δt (s) | Re |
|-----------|----------------|-----|
| 32.1 | 2.4 | 16 |
| 28.7 | 2.1 | 48 |
| 25.5 | 1.7 | 78 |
| 21.4 | 1.4 | 110 |

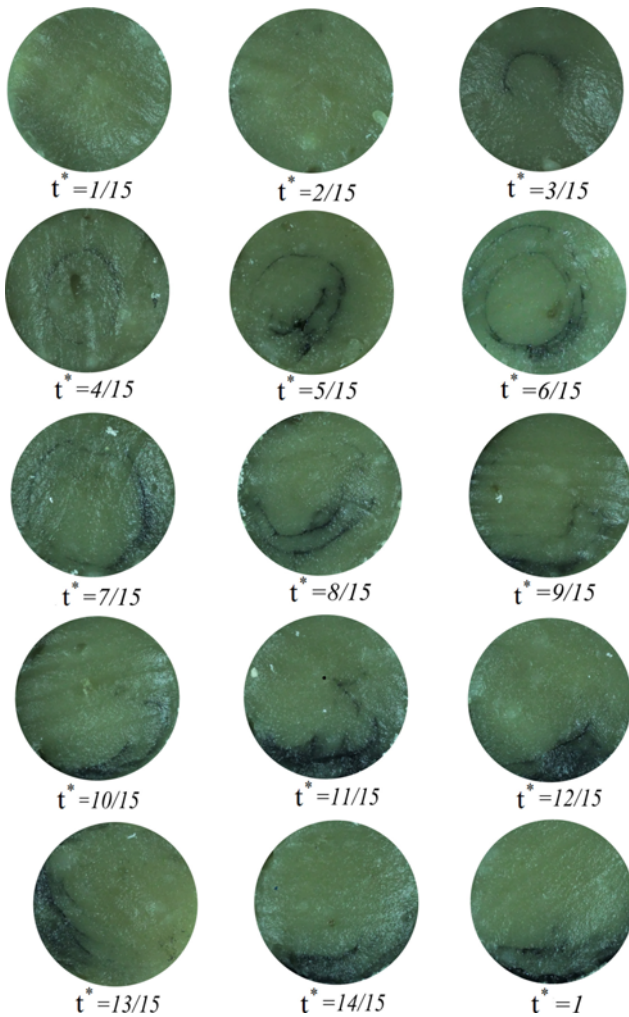


Fig. 12. Images for samples at $Re=16$ of the dough mixer (The dye has black color which its distribution illustrates mixing performance).



Fig. 13. Poor mixing at $Re=16$.

adequately; it exhibited fluid extension leaving the apparatus at $Re=16$. Fig. 13 shows that the injected dye showed no significant transverse motion; thus no folding occurred. The ingredient particles would not go far in the width of the flow.

To investigate the mixing performance, the mixing of the colored fluid was quantitatively determined using image processing. Fig. 14

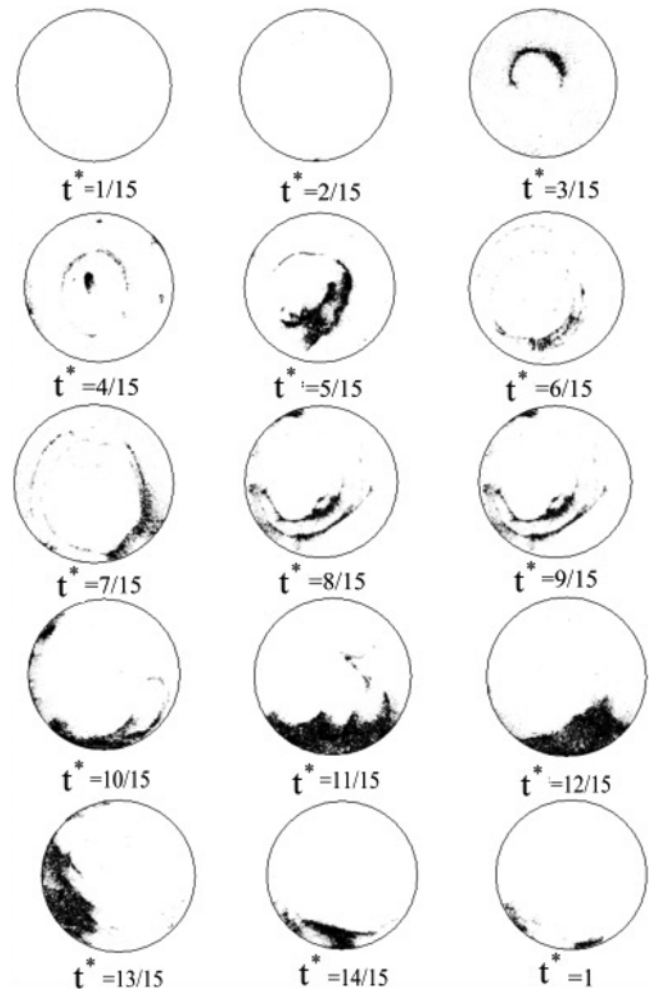


Fig. 14. Processed images for samples at $Re=16$.

shows processed images at $Re=16$.

Processed image at $Re=78$ is illustrated in Fig. 15. Mixing is much better at $Re=78$ so that $t^*=4/15$ shows portions of the injected fluid. The scatter of these portions is gradually increased and projected to larger volumes of the samples. Some of the injected fluid can reach the central flow in this case.

Processed images at $Re=110$ are demonstrated in Fig. 16, which shows that the best mixing occurs at $Re=110$. The injected dye reaches the central flow at this rotation speed and the scattering continues to larger volumes of the samples. This can be due to continuous elongation and folding of the injected elements of fluid that distribute these elements transversely. This scattering reaches its maximum values in $t^*=9/15$. The intensity of the black spots decreases because of lower concentration of the injected fluid. An interesting observation in the last t^* is the formation of colored regions next to the wall, which can be attributed to contact between injected fluid and whole internal circumference of the wall. The ingredient particles go far away in width of the flow, which indicates sensitivity of these particles to the initial conditions. These are the necessary and sufficient conditions for making a chaotic advection.

5. Mixing Index

Mixing index, which was employed to quantify the mixing performance, is defined as the ratio of number of colored pixels to the

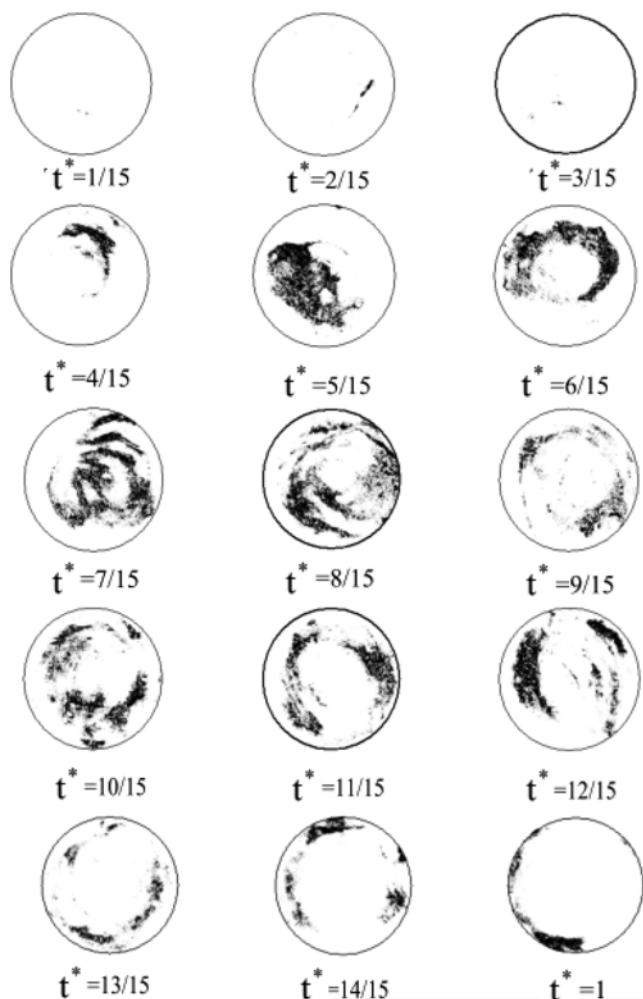


Fig. 15. Processed images for samples at Re=78.

number of total pixels (Eq. (4)). Mixing index versus dimensionless time is sketched in Fig. 17.

$$\text{Mixing index} = \frac{\text{Number of colored pixels}}{\text{Number of total pixels}} \times 100 \quad (4)$$

The best and worst mixing indices belong to Re=110 and Re=16, respectively. Average mixing indices for Re=16, 48, 78 and 110 are reported as 6.11, 8.3, 12.3 and 17.18, respectively. Mixing at Re=48 and 78 is about 27 and 50% better than mixing at Re=16, respectively, whereas the mixing index of Re=110 is 64% greater than that of Re=16. This implies that increasing the rotation speed significantly improves mixing.

Increasing the angular velocity will result in a higher momentum and make particles move faster, which therefore increases the mixing of the fluid. Since the mixer studied in this research behaves chaotically, the angular velocity of the rotor affects the mixing process more noticeably compared to other types of mixers. Increasing the rotor velocity will lead to more particle divergency in a shorter time. As the particles spread, the fluid elements will stretch and fold. In addition, increase of the resulted exponential interface will significantly improve the mixing.

Chaotic mixing is characterized by an exponential rate of stretching the fluid elements. When a fluid element passes through a chaotic

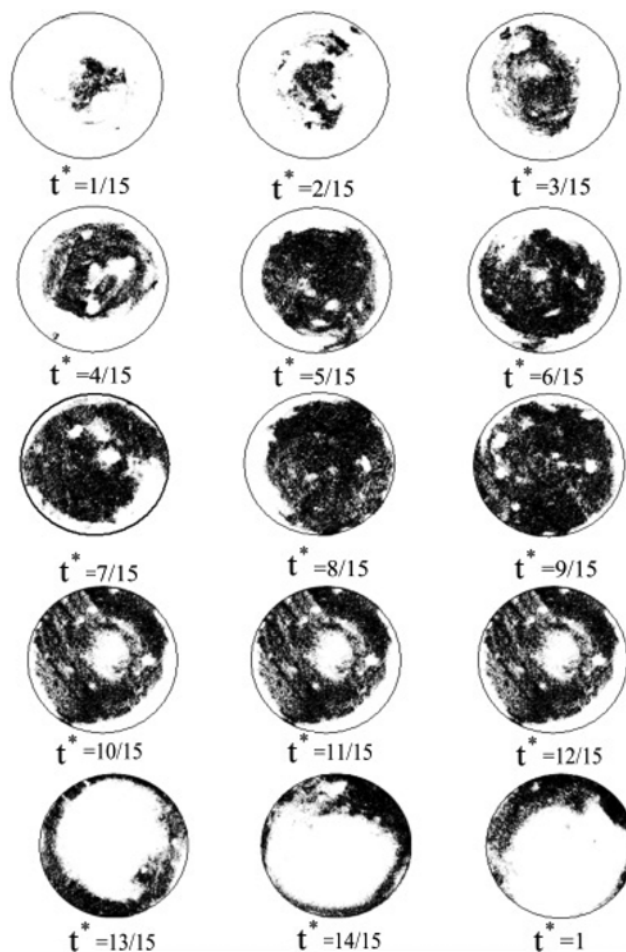


Fig. 16. Processed images for samples at Re=110.

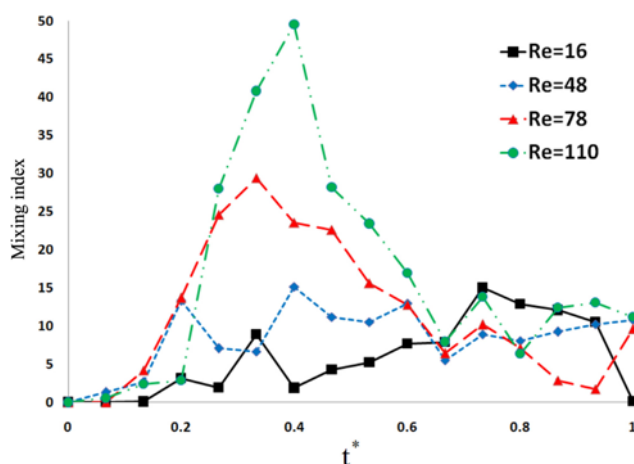


Fig. 17. Mixing index versus dimensionless time.

flow, it not only stretches but also changes direction due to sequential changes in the direction of the flow field applied on it. The change in direction causes the material lines to be folded. Repeating the cycles of stretching and folding of the material increases the area of the material medium exponentially.

6. Stepwise Motion

The flow of fluids with low speed or high viscosity is usually

laminar and steady. These types of processes are weak mixing media because the fluid motion is described by linear viscous forces rather than nonlinear inertial ones. If the applied force is time dependent, the fluid particles could follow concentrated and closed streamlines. From a mixing point of view, lack of local dependence to time leads to poor performance. Diffusion in viscous materials is minimum, since permeability is usually low, and mixing time needed for achieving homogeneity in many applications is too long via permeability [30].

Since the viscosity of dough is significantly high, the Reynolds number is very small in this model. Therefore, the flow is considered to be creeping flow. An important issue in the creep flow is the kinematic reversibility. In other words, the flow will be reversed in all points if the boundary conditions are reversed. Reversibility of the Stoke's flows will actually lead to a heterogeneous mixing between two viscous fluids.

Chaotic mixing systems are effective because, in Lagrangian mode, they associate mixing process with time. Chaotic mixing is characterized by an exponential rate of stretching of the fluid elements. When a fluid element passes through a chaotic flow, it is not only stretched but changes direction due to sequential changes in the direction of the applied field. These changes in direction would cause the material lines to fold [30].

The literature contains studies of a number of chaotic mixers [6, 7,9-11] that use temporally periodic perturbation to create chaotic advection. To study the effect of the time-dependent movement of the rotor on mixing, a rotor with stepwise motion protocol is examined experimentally. To compare different effective parameters of step motion (i.e., amplitude of movement and period), four tests at the same mean rotational speed of Ω were implemented. For this

time-periodic flow, the period T_p was taken as (see Table 3).

Fig. 18 shows the mixing parameters versus dimensionless time in these four experiments. As seen, step motion improves mixing behavior such that the averaged efficiency of mixing for constant speed movement is about 13% lower than that of step-wise movement (test 2).

The improved mixing can be attributed to the rotor acceleration during speed alteration transfers to the fluid particles. These accelerated movements provide better conditions for mixing. To investigate the effects of amplitude of movement on mixing behavior, one can consider mixing indices (Eq. (4)) of tests (2) and (3) which were processed for $\Omega_{max}/\Omega_{min}=1.3$ and 2.75, respectively.

Comparing this pair of profiles clarifies that an increased amplitude ratio can improve the mixing index; thus, increasing the amplitude ratio from 1.3 to 2.75 can raise the averaged mixing index from 10.26 to 13.04, an approximate 21% growth.

Another important parameter which affects the kinetics of the flow and mixing is time period length. One can notice the effect of time period on mixing by comparing the mixing index diagrams of tests (3) and (4). Increasing the period from 10s (test 4) to 20 s (test 3) altered the mixing index from 10.44 to 13.04, which is about 20% growth.

Results showed that increasing the time period T_p leads to increase of the mixing performance. When T_p is equal to fluid 10 s, time-dependent perturbation develops very rapidly in the flow field due to high viscosity and low diffusivity. Time-dependent perturbation generates significant chaotic mixing through inertial perturbation of streamlines. Increasing T_p to 20 s enhances the stretching and folding mechanism. Repeating cycles of stretching and folding increases the material interface generation exponentially and, consequently, increases mixing at an exponential rate.

CONCLUSIONS

We studied the laminar mixing of highly viscous fluids in a continuous chaotic mixer. To investigate the mixing performance, the effects of the constant and stepwise rotor's angular velocity on mixing efficiency were examined.

Our tests indicate that increased rotation speed has positive effects on the performance of the apparatus, such that at rotation speeds greater than 30 rpm appropriate mixing is ensured. Very low rotation speeds result in poor mixing due to insufficient transversal motion of the flow as the fluid's elements are only stretched and not folded. Observations at high rotation speeds showed that injected colored particles reach the center of the flow more as a result of transversal movement. Stretching of the fluid's elements occurs along with folding as signs of chaotic advection.

To study the effect of the time-dependent motion of the rotor on mixing, we ran a rotor with stepwise motion protocol. Results showed that step motion improves by about 10% the mixing performance compared to constant speed operation. To investigate the effects of the amplitude of stepwise movement on mixing performance, one can consider mixing indices for $\Omega_{max}/\Omega_{min}=1.3$ and 2.75. Results show that increasing the amplitude ratio from 1.3 to 2.75 improves the averaged mixing index by 20%. Another important parameter which affects the kinetics of flow and mixing is length of the time period. Increasing the period from 10 s to 20 s leads to improve-

Table 3. Rotation speed of in step motion

| Test | Ω_{min} (rpm) | Ω_{max} (rpm) | $\Omega_{max}/\Omega_{min}$ | T_p (s) |
|------|----------------------|----------------------|-----------------------------|-----------|
| 1 | 15 | 15 | 1 | - |
| 2 | 13 | 17 | 1.3 | 20 |
| 3 | 8 | 22 | 2.75 | 20 |
| 4 | 8 | 22 | 2.75 | 10 |

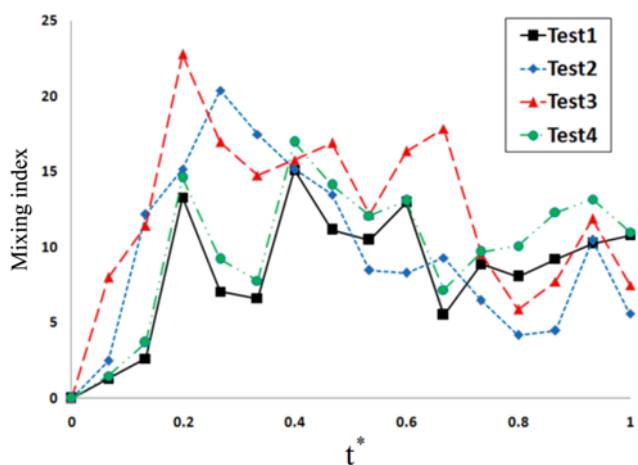


Fig. 18. Mixing index versus dimensionless time in step motion rotor experiments.

ment of 20% in mixing performance.

REFERENCES

1. R. K. Connelly and J. L. Kokini, *J. Food Eng.*, **79**, 956 (2007).
2. R. K. Connelly and J. L. Kokini, *J. Food Process Eng.*, **22**, 435 (1999).
3. S. Kumar and G. M. Homsy, *Phys. Fluids*, **8**, 1774 (1996).
4. A. Lefevre, J. P. B. Mota, A. J. S. Rodrigo and E. Saadjan, *Int. J. Heat Fluid Flow*, **24**, 310 (2003).
5. R. H. Liu, M. A. Stremmer, K. V. Sharp, M. G. Olsen, J. G. Santiago, R. J. Adrian, H. Aref and D. J. Beebe, *J. Microelectromech. Syst.*, **9**, 1059 (2000).
6. W. L. Chien, H. Rising and J. M. Ottino, *J. Fluid Mech.*, **170**, 355 (1986).
7. K. C. Miles, B. Nagarajan and D. A. Zumbrenen, *J. Fluids Eng.*, **117**, 582 (1995).
8. C. Sadhan, J. Tjahjadi and J. M. Ottino, *AIChE J.*, **40**, 1769 (1994).
9. P. D. Swanson and J. M. Ottino, *J. Fluid Mech.*, **213**, 227 (1990).
10. T. C. Niederkorn and J. M. Ottino, *J. Fluid Mech.*, **256**, 243 (1993).
11. T. Atobe, M. Funakoshi and S. Inoue, *Fluid Dynamics Research*, **16**, 115 (1995).
12. N. Acharya, M. Sen and H. Chang, *Int. J. Heat Mass Transfer*, **35**, 2475 (1992).
13. A. Mokrani, C. Castelain and H. Peerhossaini, *Int. J. Heat Mass Transfer*, **40**, 3089 (1997).
14. C. Chagny, C. Castelain and H. Peerhossaini, *Appl. Therm. Eng.*, **20**, 1615 (2000).
15. M. J. Clifford, S. M. Cox and M. D. Finn, *Chem. Eng. Sci.*, **59**, 3371 (2004).
16. H. Peerhossaini, C. Castelain and Y. Le Guer, *Exp. Therm. Fluid Sci.*, **7**(4), 333 (1993).
17. C. Castelain, A. Mokrani, Y. Guer and H. Peerhossaini, *The European Journal of Mechanics-B/Fluids*, **20**, 205 (2001).
18. T. C. G. O. Fountain, D. V. Khakhar, I. Mezic and J. M. Ottino, *Chem. Eng. Sci.*, **417**, 265 (2000).
19. D. J. Lamberto, M. M. Alvarez and F. J. Muzzio, *Chem. Eng. Sci.*, **56**, 4887 (2001).
20. G. Metcalfe and D. Lester, *J. Food Eng.*, **95**, 21 (2009).
21. J. Chaiken, R. Chevray, M. Tabor and Q. Tan, *Proc. R. Soc. Lond. A*, **408**, 165 (1986).
22. J. Chaiken, C. K. Chu, M. Tabor and Q. M. Tan, *Phys. Fluids*, **30**, 687 (1987).
23. H. Aref and S. Balachandar, *Phys. Fluids*, **29**, 3515 (1986).
24. T. C. Niederkorn, M. Julio and J. M. Ottino, *AIChE J.*, **40**, 1782 (1994).
25. S. M. Hosseinalipour, A. Tohidi, M. Shokrpour and N. M. Nouri, *J. Mech. Sci. Technol.*, **27**(5), 329 (2013).
26. D. M. Binding, M. A. Couch, K. S. Sujatha and M. F. Webster, *J. Food Eng.*, **58**, 111 (2003).
27. K. S. Sujatha, M. F. Webster, D. M. Binding and M. A. Couch, *J. Food Eng.*, **57**, 67 (2003).
28. K. M. Dhanasekharan and J. L. Kokini, *J. Food Eng.*, **60**, 421 (2003).
29. P. J. Cullen, *Food mixing: Principles and applications*, Wiley-Blackwell (2009).
30. E. L. Paul, V. Atiemo-Obeng and S. M. Kresta, *Handbook of industrial mixing: Science and practice*, Wiley-Interscience (2003).